Experimental Investigation and Modeling of Denitrification of Water in a Column Bioreactor Using Immobilized Microorganisms on Modified Zeolite

Ehsan Zamani Abyaneh ⓘ**, Mohammadhosein Heidary** ⓘ**, Mahkame Rafaatinia** ⓘ**, Arash Darzian Rostami** ⓘ**, Fatemeh Yazdian*** ⓘ**, Behnam Rasekh** ⓘ**, Navid Mostoufi**
** ⓘ

1. Process Design and Simulation Research Center, School of Chemical Engineering, College of Engineering, University of Tehran, Tehran, Iran. E-mail: ehsanzamani@ut.ac.ir
2. Process Design and Simulation Research Center, School of Chemical Engineering, College of Engineering, University of Tehran, Tehran, Iran. E-mail: heidary.mohamad@ut.ac.ir
3. Process Design and Simulation Research Center, School of Chemical Engineering, College of Engineering, University of Tehran, Tehran, Iran. E-mail: mahkame.r89@gmail.com
4. Department of Life Science Engineering, Faculty of New Science and Technologies, University of Tehran, Tehran, Iran. E-mail: arashrostami91@gmail.com
5. Department of Life Science Engineering, Faculty of New Science and Technologies, University of Tehran, P.O. Tehran, Iran. E-mail: yazdian@ut.ac.ir
6. Microbiology and Biotechnology Research Group, Research Institute of Petroleum Industry, Tehran, Iran. E-mail: b.rasekh@gmail.com
7. Process Design and Simulation Research Center, School of Chemical Engineering, College of Engineering, University of Tehran, Tehran, Iran. E-mail: mostoufi@ut.ac.ir

ARTICLE INFO	ABSTRACT
	The nitrate removal efficiency of a 9.5 L packed bed column bioreactor was evaluated using different feeding strategies and initial concentrations. The bioreactor was filled with zeolite mineral particles and initially treated with Thiobacillus denitrificans. Several hydraulic retention times were examined to assess the effectiveness of nitrate removal. The most favorable scenario resulted in an 87% reduction in nitrate concentration from an influent of 400 mg/L within a three-hour period. To determine the optimal length of the bioreactor, a computational fluid dynamics model was developed. By comparing simulations with experimental results, the ideal height of the bioreactor for complete denitrification was determined to be 90 cm, 45 cm, 30 cm, and 20 cm for influents with nitrate concentrations of 400 mg/L, 250 mg/L, 120 mg/L, and 80 mg/L, respectively.

Introduction

Nitrate is the most common pollutant in water resources of ecosystems. Moreover, its inputs to the environment have been on the rise for the past few decades [1], making the availability of a sustainable source of healthy water increasingly important to many countries because of

---

the increasing population, expansion of industries, and climate change effects. Various methods are available for nitrate removal from water, such as reverse osmosis, ion exchange, electrodialysis, and membrane processes [2-5]. Additionally, there is a rising interest in biological methods [6]. One significant aspect of these biological approaches is microbial denitrification, a respiratory process carried out by autotrophic and heterotrophic microorganisms [7].

The majority of denitrifying microorganisms are heterotrophs, relying on complex organic substances like methanol, ethanol, methane, carbon monoxide, and acetic acid as electron donors for the conversion of nitrate to nitrogen [8]. Additionally, some researchers have utilized natural materials like wheat straw and plant wood as sources of organic carbon for heterotrophic denitrification. While this method is cost-effective, it comes with a lengthy and intricate pre-treatment process. In practical applications, for the removal of nitrate from drinking water, simple and readily degradable substrates like methanol, ethanol, and acetic acid are predominantly utilized [9].

A diverse array of autotrophic bacteria finds application in the denitrification of water with minimal organic matter content. These microorganisms utilize an inorganic carbon source, such as CO_2, as their carbon source [9]. Their advantage lies in not necessitating an external organic substrate, making them a more cost-effective option [10]. Furthermore, these microorganisms yield low biomass, thereby minimizing the risk of contamination [1].

Sulfur-based autotrophic denitrification is a type of denitrification wherein elemental sulfur, hydrogen sulfide, or thiosulfate serves as electron donors. Certain properties of sulfur make it well-suited for denitrification, such as its non-toxic nature, insolubility in water, and stability under normal conditions [10]. However, a few species of microorganisms are capable to reduce nitrate through oxidizing sulfur elements (S^{2-}, $S_2O_3^{2-}$, SO_3^{2-}) [11-14]. A number of researchers have studied the autotrophic denitrification process by Thiobacillus denitrificans (enriched sludge or pure culture) for the removal of nitrate from drinking water, groundwater, and wastewater using reduced sulfur compounds as electron donors [10, 15-19]. However, only a limited number of studies have investigated the effectiveness of immobilized Thiobacillus denitrificans Immobilization has the potential to improve denitrification efficiency and safeguard the bacteria from adverse environmental conditions. The colonization and activation of denitrifying bacteria communities on supports are critical factors to obtain high denitrification efficiency [20]. Denitrificans can perfectly grow in a packed bed reactor, where the biofilm grows around the fixed carrier comprised of porous organic matter or mineral matrixes formed by large surface area particles [1]. There have been many different materials used as bacteria supports in the past, such as metal oxides [21, 22], zeolites [23], biodegradable polymers [24], woods [25], or carbon materials [26]. Organic supports, such as polymers, pose various challenges, including issues related to stability and disposal [27]. Conversely, inorganic materials like silica and alumina exhibit thermal and mechanical stability, along with robust strength [27]. Furthermore, Battista-Toledo et al. [28] found that different inorganic materials, like ZSM5, 13X, and b-zeolite, perform well as bacterial supports for a heterotrophic bacteria called Escherichia coli.

In addition to the characteristics of the supports, environmental parameters such as C/N ratio, temperature, and pH of polluted water influence the community structure and activity of denitrifying bacteria. There are several investigations [6, 7, 9, 29-34] on the denitrifying bioreactors. Torrentó et al. [35] found that nitrate input concentration plays an essential role in the denitrification efficiency of the reactor. Nitrate removal improves by lowering the initial nitrate concentration and grain size. According to Carrera et al. [36], denitrification is more efficient at high temperatures rather than at low temperatures. However, even at low temperatures, the desired nitrate removal efficiency can be achieved by increasing the hydraulic

retention time (HRT). This parameter is a significant factor that should be considered during the design of a reactor. In a heterotrophic system, HRT is adjusted based on the growth rate of microorganisms, initial nitrate concentration, presence of other inhibitory species, and temperature [9].

This work aims to investigate the effectiveness of Clinoptilolite zeolite particles as a support for Thiobacillus denitrificans as well as evaluate the performance of a 9.5 L pilot-scale bioreactor filled with Clinoptilolite zeolite mineral for denitrification process. Furthermore, a computational fluid dynamics (CFD) model is developed using COMSOL 5.4 software in an attempt to investigate what the optimal length of the bioreactor would be for a desired HRT. CFD has proven to be a promising tool to study the flow fields in a reactor and can be successfully applied for design, redesign, and scale-up purposes in the future. Taking into account the above-mentioned goals, different feeding strategies, and various initial concentrations of nitrate ions were applied at various hydraulic retention times.

Materials and Methods

Column Bioreactor

The bioreactor used for the denitrification process was a packed bed reactor which was 90% filled with Clinoptilolite zeolite particles of different sizes. Fig. 1 illustrates a schematic picture of this bioreactor, as well as how different particles were arranged inside it. An upward flow was considered for this system to prevent the accumulation of nitrogen and other gases inside the column. Therefore, the inlet to the bioreactor is located at the bottom. Deoxygenated synthetic water (by Nitrogen gas) was pumped from the feeding tank into the column, and it was treated by autotrophic denitrifying microorganisms attached to the zeolite, and exited from the top of the upper portion of the column. The bioreactor was a Plexiglas cylinder, measuring 100 cm in height and 5.5 cm in diameter (9.5 L). It can be seen in Fig. 1 that four ports for liquid samples were installed along the column at 25 cm apart from each other. In addition, two ports were considered for the sampling particles. Larger particles were placed at the bottom, and smaller ones were toward the top of the bed. Change of particle size along the column was considered to increase the contact area as the influent raises in the bioreactor, compensating for lower nitrate concentration due to the denitrification process at the bottom. The characteristics of Clinoptilolite zeolite particles are given in Table 1. Their sizes ranged between 0.4 and 6 mm and had irregular shapes. The average porosity of particles was determined to be 50% and the density ranged between 0.5 and 1.1 kg. m-3.
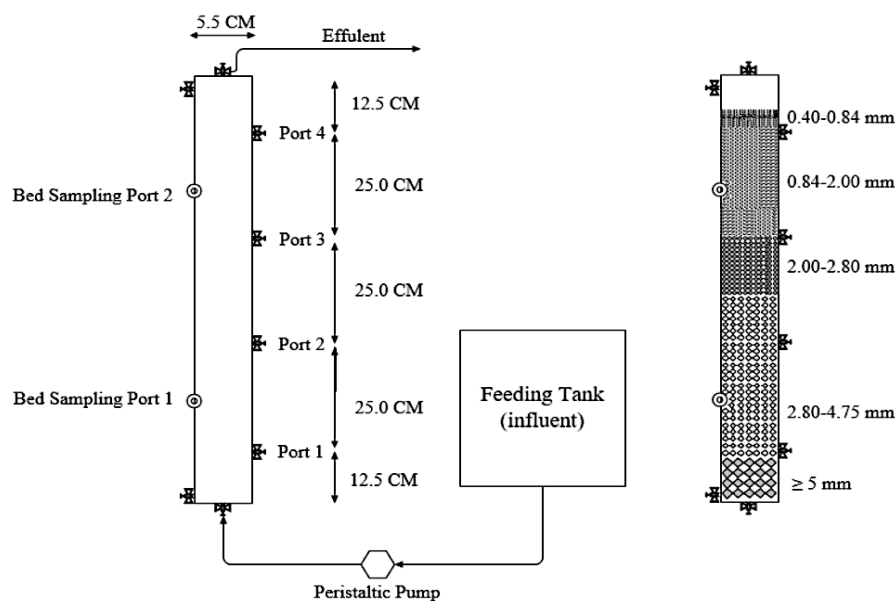
Fig. 1. Schematic of the column bioreactor and arrangement of the beds of different sizes of particles

Table 1. Properties of zeolite particles

Size (mm)	0.4 – 6
Shape	Irregular
Particle Porosity (%)	50
Density (kg/m^3)	0.5 – 1.1

Zeolite Modification

Before starting the test and in order to remove surface impurities, zeolite particles were washed with water for 48 hours and then dried in an oven at 105 °C for 48 hours. Then, 20 vol.% hydrochloric acid was applied for four hours, followed by extensive washing with distilled water until pH 6 was reached in the effluent. The particles were then dried in an oven at 105 °C for 48 hours. The color of zeolite became brighter after modification by acid.

Microbiological Culture

This investigation was part of a bigger plan for denitrification of water containing nitrite and sulfur elements in large scales. In this regard, Thiobacillus microorganism (ATCC 23644 Gram-negative) was used for the simultaneous elimination of nitrite and sulfur. The microorganism was obtained from the German DSMZ microbial collection. This microorganism utilizes sulfur for energy (hydrogen sulfide, elemental sulfur, or thiosulfate) and requires a pH of 7 and a temperature of 30 °C for optimum growth. Thiobacillus denitrificans were cultivated on a basal salt medium (BSM) which was prepared in three separate and isolated parts. The composition of BSM is presented in Table 2. Compounds containing phosphorus and chlorine were esterified separately. An autoclave was used to sterilize all the ingredients of the culture medium for 20 minutes at 121 °C and 1.5 atm pressure. Once the sterile solutions were removed from the autoclave, they were cooled down to 50 °C, mixed together, and divided into sterile vials. The strains were mixed using a flame and sterilized syringe under the biological hood, then inoculated into the vials at a rate of 10% and incubated at 30 °C for one week. The stored microorganism cultures were transferred to the new environment on a monthly basis and the new cultures replaced the previous ones. To avoid interference from photoautotrophic microorganisms, aluminum foil was used to cover the column, preventing the penetration of light into the system.

Table 2. BSM compositions

Chemical Formula	Amount
KH_2PO_4	1.8 (g/L)
Na_2HPO_4	1.2 (g/L)
$MgSO_4.7H_2O$	0.1 (g/L)
$(NH_4)_2SO_4$	0.1 (g/L)
$CaCl_2.2H_2O$	0.03 (g/L)
$Na_2S_2O_3.5H_2O$	15 (g/L)
$FeCl_3.6H_2O$	0.02 (g/L)
$MnSO_4$	0.02 (g/L)
$NaHCO_3$	0.5 (g/L)
KNO_3	5 (g/L)
EDTA	0.0005 (g/L)
$ZnSO_4.7H_2O$	0.0001 (g/L)
$CuCl_2.2H_2O$	0.00001 (g/L)
$MnCl_2.4H_2O$	0.00003 (g/L)
$CoCl_2.6H_2O$	0.0002 (g/L)
$Na_2MO_7O_{24}.2H_2O$	0.00003 (g/L)
$FeSO_4.7H_2O$	0.0002 (g/L)
H_3BO_3	0.0003 (g/L)
$NiCl_2.6H_2O$	0.00002 (g/L)

Operational Plan

The operating plan for this investigation is reported in Table 3. The whole operation took about 4 months, and sampling for physicochemical properties was performed 2 to 3 times per week from the designated ports. There were three phases in the operational plan, each with a different objective. Detailed descriptions of each phase are provided below.

Before starting the process and in order to reach a usable level of cell population in the column inoculation, 5 L of BSM was inoculated by Thiobacillus denitrificans. It was incubated in an Erlenmeyer flask at 30 °C under sterile conditions for 30 days. The number of cells was counted under an optical microscope to ensure the growth and division of cells. Also, every week, 10% of the medium was replaced with a fresh BSM.

Table 3. Operational plan of the column bioreactor

Stage	Target	Culture Medium	HRT (h)	Nitrate Input Concentration (mg/L)	Days
Setting up	Growth of Autotrophic Microorganisms	BSM	25	1500	1-6
			32	1500	
Growth and Incubation	Biofilm Formation	BSM/Synthetic Water	32	550	7-30
Feeding	Performance Evaluation	Synthetic Water	25	400 / 250 / 120 / 80	31-44
			15	400 / 250 / 120 / 80	45-61
			12	400 / 250 / 120 / 80	62-75
			10	400 / 250 / 120 / 80	76-85
			6	400 / 250 / 120 / 80 / 1500	86-98
			3	1500 / 400 / 250 / 120 / 80	99-113

The first stage (set-up) involved adding 4 L Thiobacillus denitrificans medium from the discontinuous culture, and 6 L of non-sterile BSM to the reactor inlet. The reactor operated in a closed loop in order to provide sufficient contact time between cells, nutrients and substrate. During this period, 1 L of fresh BSM was added to an influent nitrate concentration of 550 mg. L^{-1} each day. It should be mentioned that until the 6th day (end of set-up stage), the HRT was set to 25 hours and to 32 hours afterward. The hydraulic retention time was calculated as follows:

$$HRT = \frac{Pore\ bed\ volume}{Flow\ rate} = \frac{V\varepsilon}{Q} \qquad (1)$$

where V is the volume of the bed, ε is the porosity, and Q is the flow rate.

In the growth and incubation stage, the reactor cycle was changed from closed to open to form the microbial biofilm and the column was treated with a BSM containing 550 mg. L^{-1} nitrate ion. The concentration of nitrate ions was measured each day to monitor its significant reduction in the effluent. This reduction indicated that the bioreactor was ready for the gradual replacement of BSM with synthetic water (SW). The compounds present in different concentrations of synthetic water (SW) are given in Table 4.

Table 4. components of SW for different nitrate ion concentrations (mg/L)

Nitrate Input Concentration (mg/L)	Chemical Formula						
	KNO_3	$NaHCO_3$	K_2HPO_4	NH_4Cl	$MgCl.6H_2O$	$FeSO_4$	$Na_2S_2O_3.5H_2O$
80	130	250	20	12	2	1	10
120	250	350	50	12	2	1	160
250	434	750	50	12	2	1	350
400	652	1200	50	12	2	1	550
550	901	1700	50	12	2	1	750
1500	2440	4000	50	12	2	1	2000

Finally, once the denitrification rate remained stable and the column reached the steady-state condition, feeding experiments were carried out and the performance of the column in removing nitrate ions was evaluated based on different nitrate input concentrations and HRTs. The feeding experiments started from the longest hydraulic retention time (25 hours) and shorter HRTs were employed based on the reactor performance and standard limits for nitrite and nitrate ions in the effluent. It is worth mentioning that with increasing nitrate ion concentration, alkaline and thiosulfate ion values also increase. ‹Therefore, the pH of the environment was adjusted in the range of 7.7-8 using 2 molar NaOH solution.

Physicochemical Analyses

Nitrate Test

In this study, the Chromotropic Acid method was employed to quantify nitrate levels, with the specified range for nitrogen being 1-130 mg. L^{-1}. The underlying principle of this method involves the creation of a yellow solution through the reaction of Nitrate Reagent A and Nitrate Reagent B with nitrate. Subsequently, the absorbance of the resulting solution was measured using a spectrophotometer at a wavelength of 410 nm. To establish the nitrate standard curve, varying concentrations of nitrate solution were prepared using potassium nitrate. Each test tube containing Nitrate Reagent A received 1 ml of nitrate solution, and the tube was shaken 10 times. Following that, Nitrate Reagent B was added to each tube through a funnel, and the tubes were shaken another 10 times. Once the yellow color fully developed, a specific volume of the solution was withdrawn using a Pasteur pipette and transferred to the cuvette. The device was initially calibrated with nitrate-free distilled water, and the absorbance of each test tube was then read at a wavelength of 410 nm to establish the nitrate standard curve.

To measure nitrate in the samples after obtaining the nitrate standard curve, cells were separated from the culture medium through centrifugation at 5000 rpm for 20 minutes. After passing the samples through a 0.45-micron filter paper and conducting the dilution process, one

milliliter of the resultant solution was transferred to a test tube containing Nitrate Reagent A, followed by 10 shakes. Subsequently, Nitrate Reagent B was introduced into the test tube using a funnel, and the tube was shaken another 10 times until the yellow color fully manifested. Spectrophotometer data and absorbance changes were then compared with the absorption standard curve, ultimately yielding the nitrate concentration.

Nitrite Test

To quantify nitrite levels, the USEPA Diazotization method was employed with a measurement range of 0.002-0.03 mg. L^{-1} of nitrogen. The methodology involves creating nitrite solutions using sodium nitrite at various concentrations. Subsequently, Nitrite Reagent is introduced to 10 ml of these solutions using a funnel, followed by shaking the tubes 10 times. After approximately 20 minutes, a pink coloration develops. A specific volume of the solution is then extracted using a Pasteur pipette and transferred to a cuvette. The instrument is initially calibrated to zero using distilled water devoid of nitrite. Subsequently, the absorbance of the samples is read at a wavelength of 507 nm, and a nitrite standard curve is generated. The method relies on the reaction of nitrite with sulfonic acid, forming diazonium salt and producing a pink color. After establishing the nitrite standard curve, cells were separated from the culture medium via centrifugation at 5000 rpm for 20 minutes. Following filtration through a 0.45-micron filter paper and necessary dilution steps, 10 mL of the upper solution was combined with the Nitrite Reagent using a funnel. After shaking the tubes and the complete development of the pink color, the absorbance of the samples was measured at a wavelength of 507 nm. Spectrophotometer data and absorption changes were then compared with the absorption standard curve to determine the nitrite concentration.

pH Test

The pH of the samples was instantly measured using a digital pH meter, without filtration or dilution, immediately after sampling.

Characterization of Zeolite Particles

In order to characterize the zeolite particles used in the research, scanning electron microscope (SEM) images were used to study the surface structure and morphology. Also, to determine the elemental composition of samples, energy dispersive X-ray (EDX) method was used at room temperature. In this method, the surface of the sample is bombarded by an electron beam inside the microscope, and when the electrons of this beam collide with the electrons of the atoms of the sample under investigation, some of these electrons are displaced. Due to the fact that the place of atoms cannot remain empty and must reach the equilibrium state, electrons from higher atomic layers migrate to this empty place and fill its place. In order to perform this action, the electrons of the higher layers, which have more energy, must lose some of their energy to reach the energy level of the new layer and be stable, and this energy is emitted as X-rays.

The magnitude of energy emitted depends on the specific layers involved both the layer from which the electron is detached and the layer to which it migrates. Additionally, each element's X-rays emit a distinct amount of energy during the transition from one atomic layer to another. Consequently, by quantifying the energy in X-rays released during electron beam bombardment, it becomes feasible to discern the type of atom within the sample. The outcome of an EDX analysis is a spectrum, where the displayed peaks are unique to individual atoms, signifying the presence of a specific element.

Computational Fluid Dynamics Model

COMSOL Multiphysics 5.4 software was utilized for generating the bioreactor configuration, meshing, and solving the governing equations using the finite element method. To obtain the flow profiles inside the bed, fluid properties were considered as water. Such an assumption is reasonable due to the low nitrate concentration in water.

Governing Equations

The governing equations for the porous fixed bed bioreactor are:

$$\frac{\partial}{\partial t}\left(\epsilon_p.\rho\right)\nabla.\left(\rho.u\right) = Q \tag{2}$$

$$u = -\frac{K}{\mu}\nabla\rho \tag{3}$$

where ϵ_p is the porosity of the bed, ρ is the density of the fluid, u is velocity, K is the permeability, and μ is the viscosity.

The equation of mass transfer for species i in the reactor, which includes diffusion, convection and chemical reaction, is as follows:

$$\frac{\partial S_i}{\partial t} + \nabla.(-D_i\nabla S_i) + \nabla.(\vec{u}S_i) = R_i \tag{4}$$

where t is time, S_i is concentration of species i, D_i is diffusion coefficient of the species i, $\vec{u}$ is velocity, and R_i is chemical reaction rate for the species i.

Reaction Kinetics

To describe the denitrification process in this study, the Monod equation was used:

$$r_s = -\frac{\mu_m S}{K_s + s} \tag{5}$$

where r_s is the growth rate of microorganism, μ_m is the maximum growth rate of microorganism, K_s is the half-velocity constant, and S is the concentration of the substrate for growth.

Model Configuration

To reach comparable results with experimental data, a 9.5 L cylindrical bioreactor was generated with the same height and diameter as actual setup. Then, the generated geometry was meshed using tetrahedral mesh elements. The generated mesh used for CFD simulations is shown in Fig. 2. As the concentration of the nitrate drops by going upward through the bioreactor, four different mesh sizes were applied ranging from coarse at the inlet to fine at the outlet to acquire precise results.

It was considered that the influent enters the bioreactor with a fixed velocity (u_0) and concentration (S_{0i}) in the simulation. The velocity was calculated based on the residence time of the fluid. Table 5 summarizes the values and parameters used for the simulation based on the experimental values. Due to the low concentration of nitrate in water, the physical properties of the fluid in the reactor were considered to be the same as water at 30 °C.
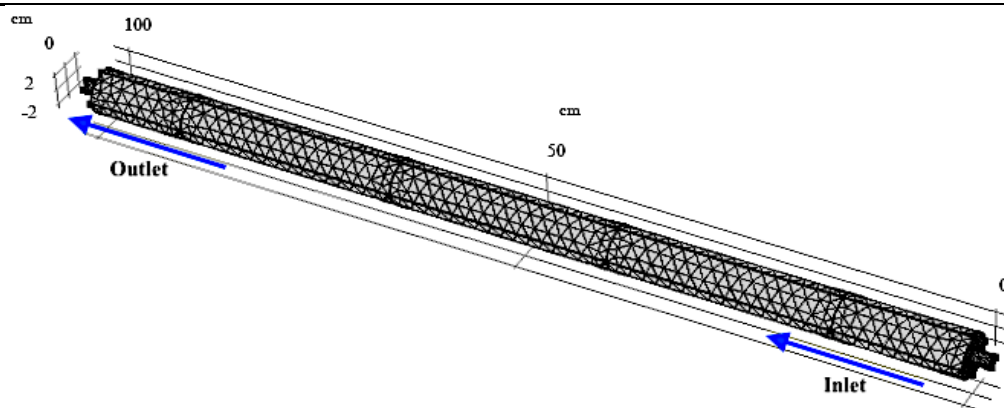
Fig. 2. Schematic of tetrahedral meshes in the bioreactor

Table 5. Parameters used in CFD simulations

Parameter	Symbol	Value	Unit
Fluid residence time	T_{av}	3	h
Nitrate molecular weight	Mw	62.0049	g/mol
Concentration of nitrate at inlet	S_0	400-80	mg/L

Results and Discussion

Zeolite Modification

The mineral morphology of water-washed zeolite, acid-modified zeolite, and zeolite-microorganism were assessed using scanning electron microscopy (SEM). Figs 3, 4, and 5 display SEM images of water-washed zeolite, acid-modified zeolite, and zeolite-biofilm, respectively, at various magnifications.
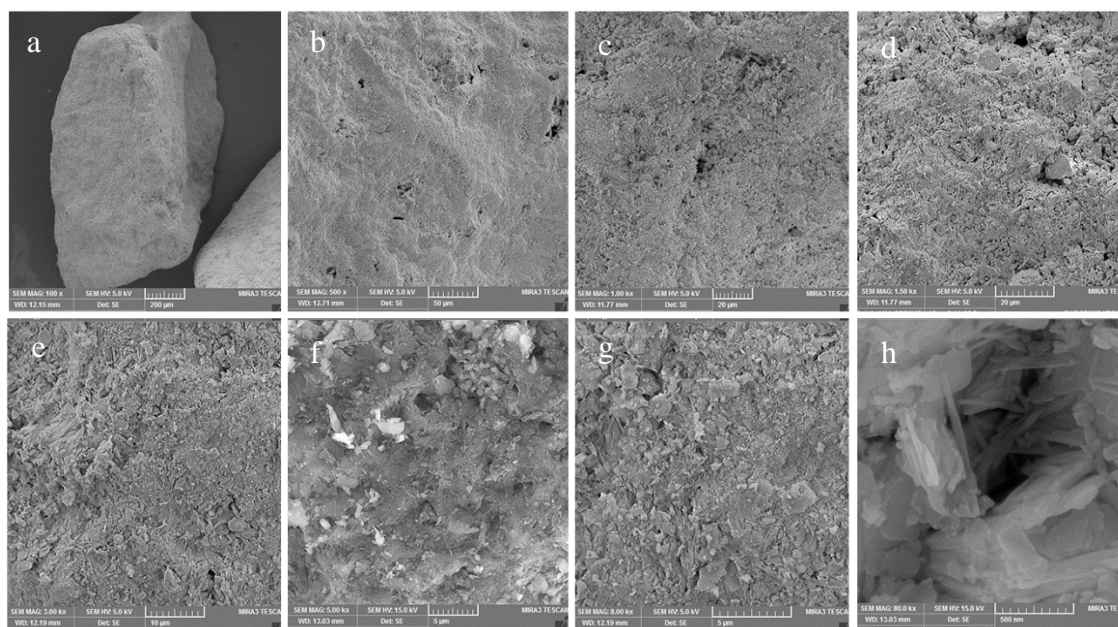
Fig. 3. SEM image of natural zeolite (a) Magnification 100, (b) Magnification 500, (c) Magnification 1000, (d) Magnification 1500, (e) Magnification 3000, (f) Magnification 5000, (g) Magnification 8000, (h) Magnification 80000
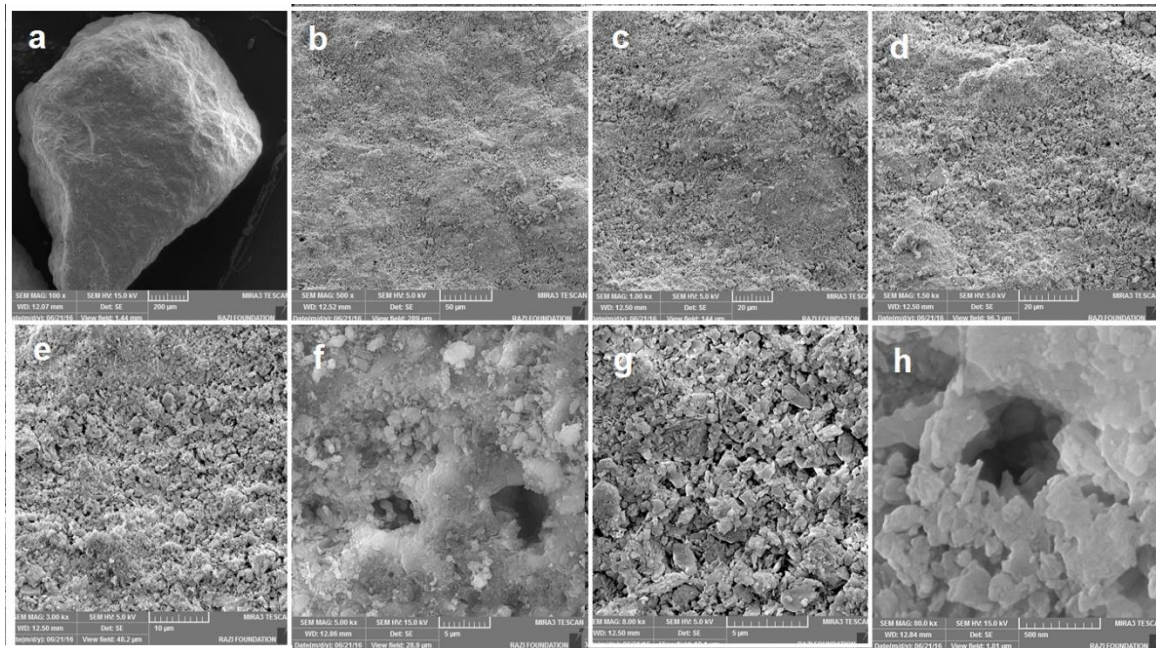
Fig. 4. SEM image of modified zeolite (a) Magnification 100, (b) Magnification 500, (c) Magnification 1000, (d) Magnification 1500, (e) Magnification 3000, (f) Magnification 5000, (g) Magnification 8000, (h) Magnification
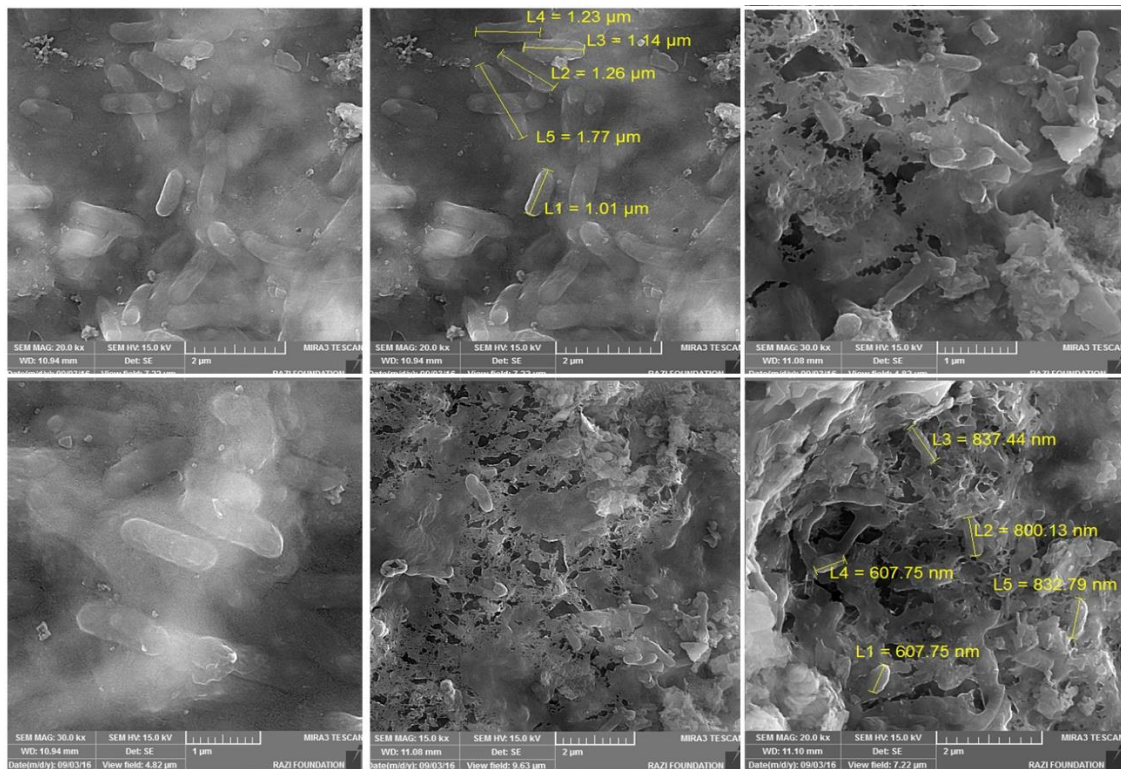
Fig. 5. SEM image of zeolite-microorganism after development of microbial biofilm

Upon comparing acid-modified zeolite with natural zeolite, it is evident that acid modification results in more significant and larger pores. This augmentation enhances the specific surface area of the zeolite, facilitating the formation of microbial biofilm. Fig. 5 presents the SEM imaging results of particles after development of microbial biofilm. As depicted in the figure, the microbial cells exhibit a bacilli shape, with lengths ranging from 0.5 to 1.4 μm, mirroring the findings of the study conducted by Gu et al. [37]. The dimensions of

the microorganisms captured in the images align entirely with those of Thiobacillus denitrificans.

Furthermore, the EDX results for both natural zeolite and modified zeolite are depicted in Figs. 6 and 7, along with corresponding data presented in Tables 6 and 7, respectively. Based on the EDX findings, the Si/Al ratio in natural zeolite is 5.45, while in acid-washed zeolite, it has increased to 11.75. In a study conducted by Shirazi et al. [38], SEM results revealed that zeolite with varying Si/Al ratios exhibits distinct morphologies and pore sizes. Surface area measurement demonstrated that reducing the Si/Al ratio leads to a decrease in the zeolite's surface area [35]. Additionally, the acidity analysis of synthetic zeolite indicated that different Si/Al ratios impact the surface acidity, which consequently impact microorganism immobilization. Therefore, the acid-modified zeolite with a higher Si/Al ratio possesses an increased surface area, enhancing the optimal conditions for biofilm formation.
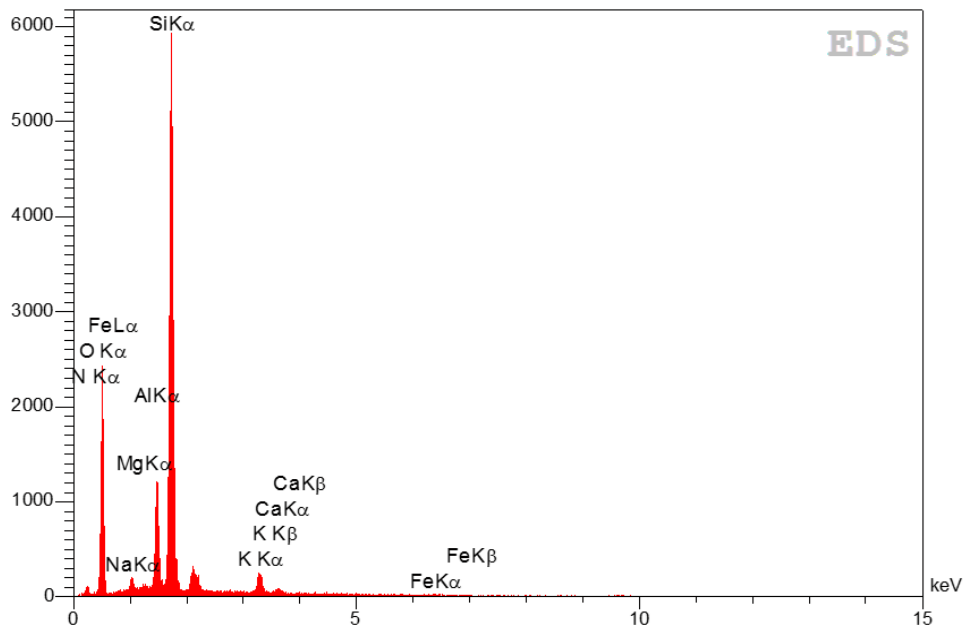
Fig. 6. EDX spectrum of natural zeolite
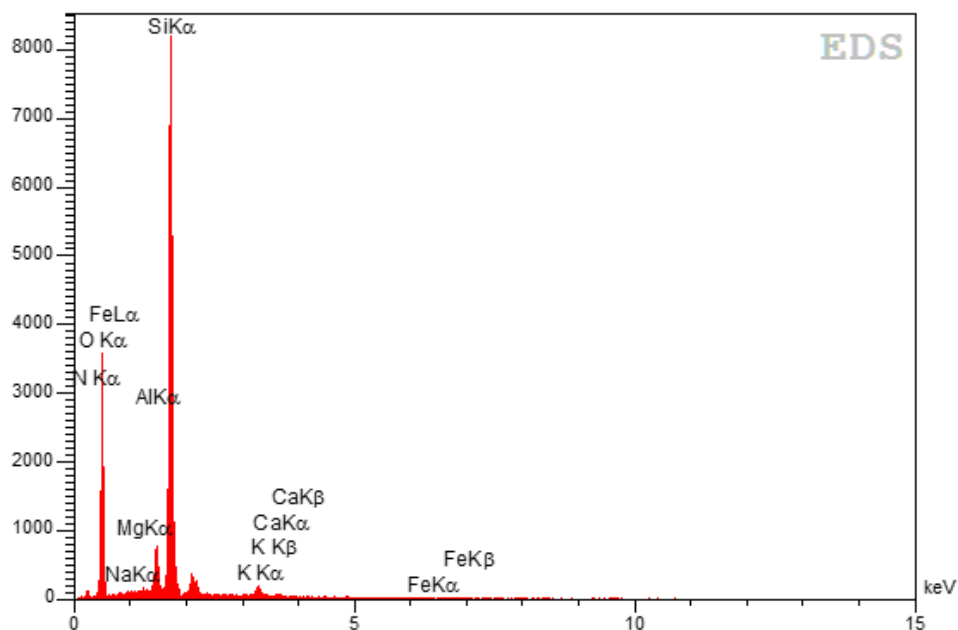
Fig. 7. EDX spectrum of modified zeolite

Table 6. Results of EDX analysis on natural zeolite

Element	Line	Int	Error	K	Kr	W%	A%	ZAF
C	Ka	12.2	3.4065	0.0259	0.0132	8.40	12.89	0.1574
N	Ka	5.5	3.4629	0.0162	0.0083	3.53	4.65	0.2343
O	Ka	360.1	3.5192	0.3740	0.1907	50.41	58.08	0.3782
Na	Ka	15.5	3.6881	0.0059	0.0030	0.58	0.47	0.5112
Mg	Ka	1.5	3.7444	0.0005	0.0003	0.04	0.03	0.6644
Al	Ka	229.0	3.8007	0.0783	0.0399	5.31	3.63	0.7523
Si	Ka	1270.0	3.8570	0.4540	0.2315	28.95	19.00	0.7997
K	Ka	58.7	0.4875	0.0365	0.0186	2.23	1.05	0.8330
Ca	Ka	4.2	0.4941	0.0029	0.0015	0.17	0.08	0.8605
Fe	Ka	3.4	0.2561	0.0057	0.0029	0.37	0.12	0.7934
				1.0000	0.5099	100.00	100.00	

Table 7. Results of EDX analysis on modified zeolite

Eelement	Line	Int	Error	K	Kr	W%	A%	ZAF
C	Ka	13.1	3.4396	0.0227	0.0118	7.38	11.17	0.1596
N	Ka	7.3	3.4964	0.0176	0.0092	3.59	4.66	0.2551
O	Ka	500.9	3.5533	0.4240	0.2201	54.65	62.10	0.4029
Na	Ka	0.0	0.0000	0.0000	0.0000	0.00	0.00	0.4998
Mg	Ka	1.1	3.7807	0.0003	0.0002	0.02	0.02	0.6578
Al	Ka	133.7	3.8375	0.0373	0.0194	2.59	1.74	0.7477
Si	Ka	1635.5	3.8944	0.4766	0.2474	30.43	19.70	0.8133
K	Ka	37.4	0.2685	0.0189	0.0098	1.18	0.55	0.8303
Ca	Ka	1.3	0.2721	0.0007	0.0004	0.05	0.02	0.8600
Fe	Ka	1.3	0.1572	0.0018	0.0009	0.12	0.04	0.7904
				1.0000	0.5192	100.00	100.00	

Experimental Measurements

Fig. 8 shows the whole denitrification process, including set-up, growth, and feeding stages with different HRTs. It also shows nitrate concentrations in the influent and effluent, and the removal efficiency during these periods. As mentioned above, during the set-up and growth stages (Fig. 8a), a constant 550 mg. L^{-1} concentration of nitrate was introduced to the bioreactor. In the set-up which lasted 7 days, the bioreactor had a negative efficiency and the concentration of nitrate in the effluent was higher than in the influent. This negative efficiency happened due to the conversion of ammonium ions into nitrate during this period. Between days 7 to 30 (the growth stage), the nitrate concentration gradually decreased in the outlet, indicating the growth and stabilization of autotrophic microorganisms in the bioreactor. Finally, the bioreactor reached an exploitation level in less than 22 days and the denitrification process could be started from this day. However, the stabilization process continued till day 30 to increase the population growth and the efficiency of the bioreactor. It is worth noting that the set-up and growth times in different systems only depend on the type and size of the bioreactor and the type of microorganisms. Thus, different times are reported in different research for these stages [15, 39, 40].

In the feeding stages (Figs. 8b to 8g), the performance of the bioreactor was tested at different HRTs (25, 15, 12, 10, 6 and 3 hours) and various nitrate input concentrations for each HRT (400, 250, 120 and 80 mg. L^{-1}). As expected, the efficiency of the bioreactor increased by lowering the input concentration in each HRT which is due to the strengthening of the biofilm and population growth on particles during the operation of the bioreactor.
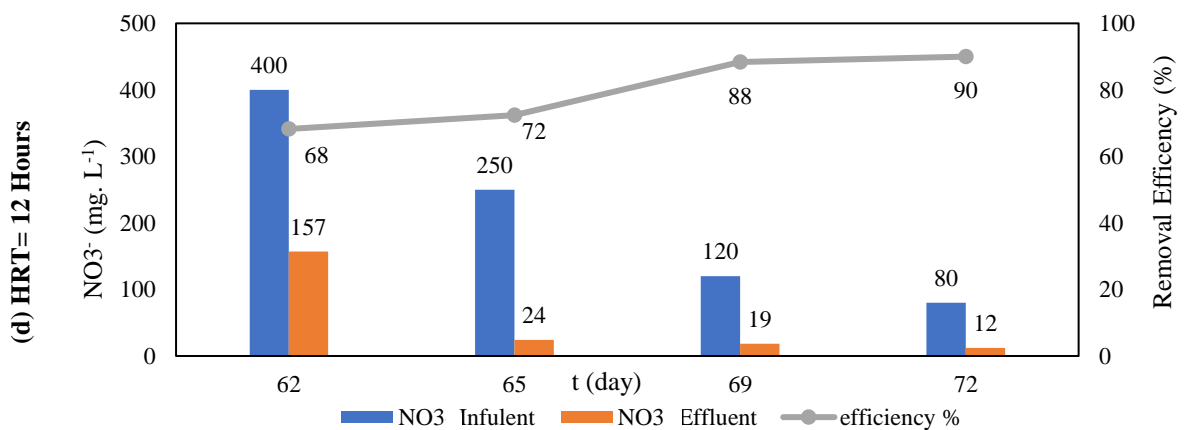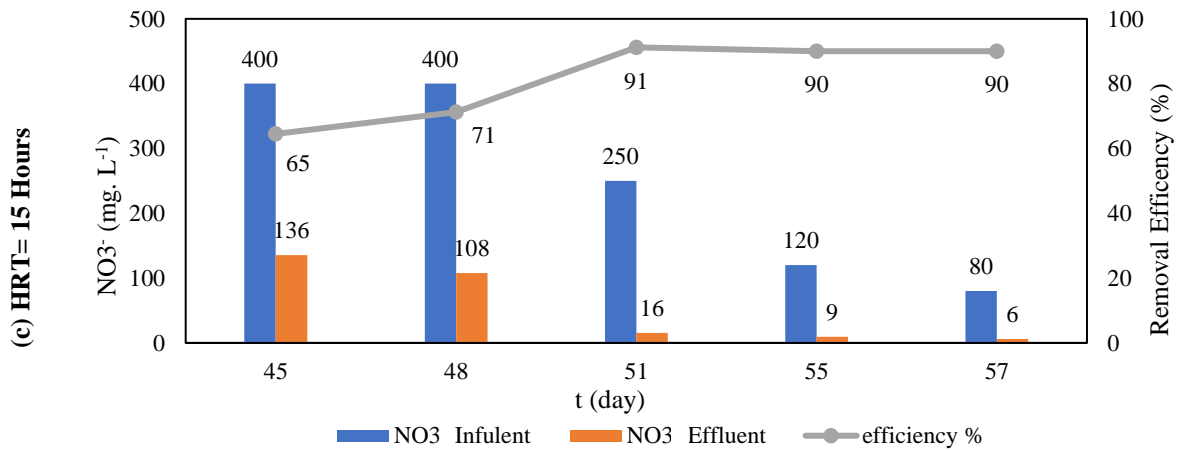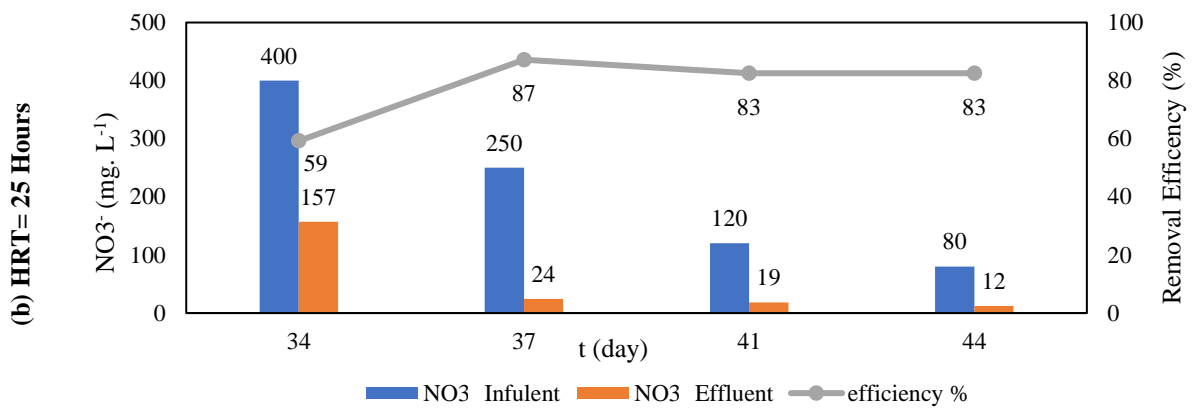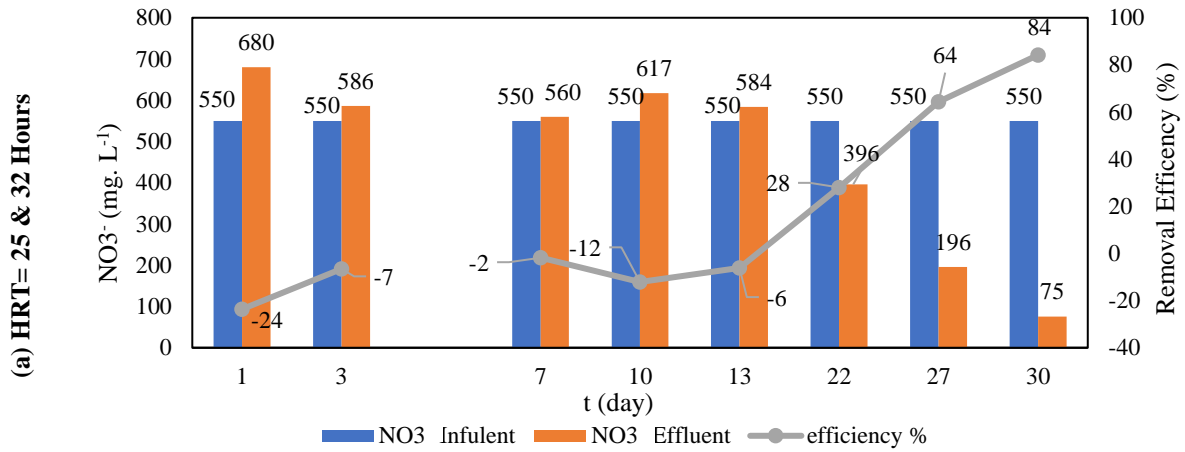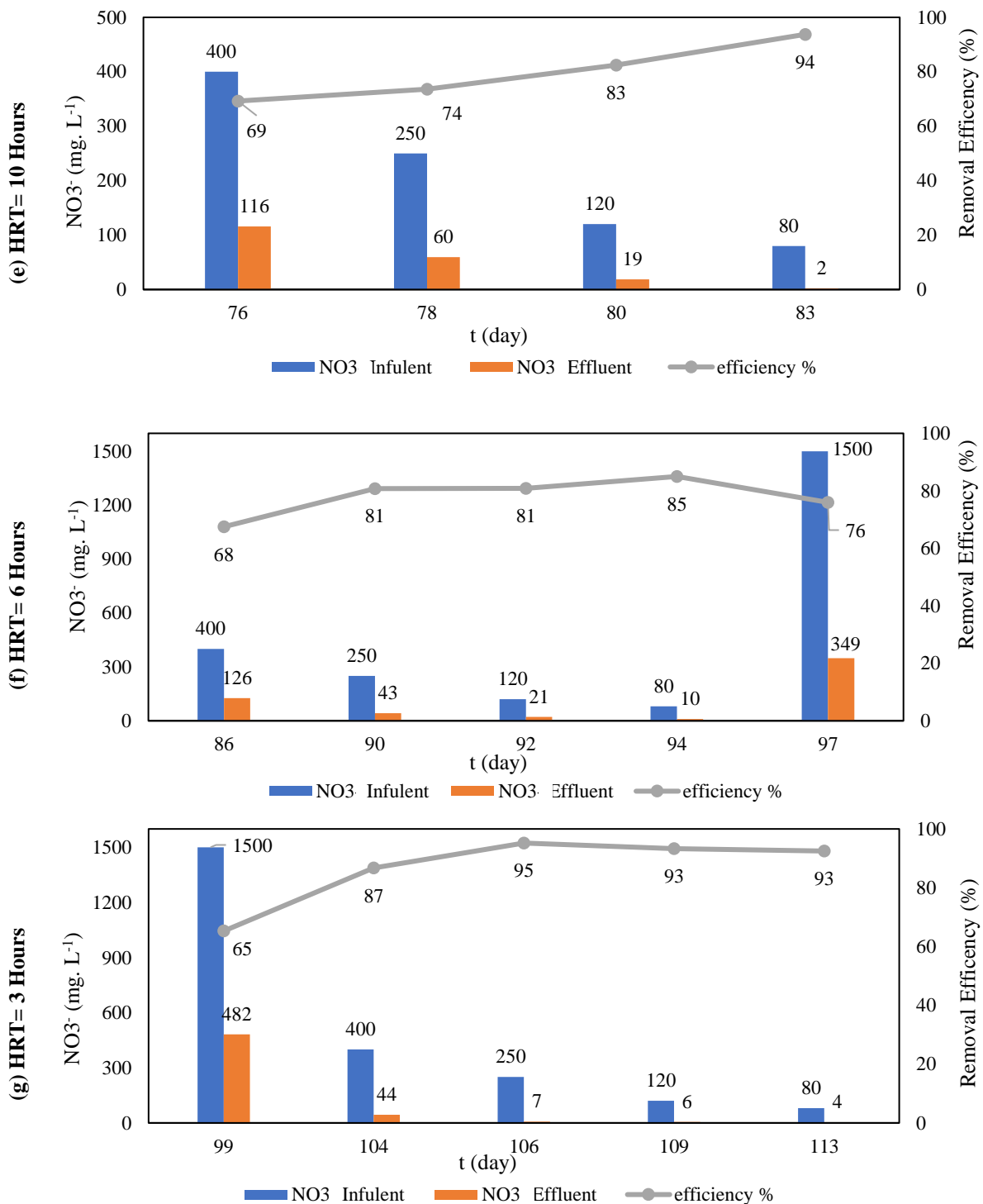
Fig. 8. Nitrate concentration and removal efficiency of the bioreactor for various HRTs, (a) set-up and growth: 25 & 32 hours, feeding: (b) feeding: 25 hours, (c) 15 hours, (d) 12 hours, (e) 10 hours, (f) 6 hours, (g) 3 hours

Comparing different HRTs, the outlet concentrations of nitrate were always below the standard value (45 mg. L^{-1}) for the influents with nitrate concentrations of 120 and 80 mg. L^{-1}. Thus, it can be said that these concentrations are less than the potential power of the bioreactor in the intended HRTs. In the case of the influent with a concentration of 250 mg. L^{-1}, the effluent nitrate concentration was always below or near the standard level in all HRTs, ensuring that higher nitrate inputs are feasible. However, for the influent with a nitrate concentration of 400

mg. L^{-1}, the efficiency of the bioreactor was considerably low, and the output nitrate concentrations were higher than the standard limit in all HRTs. To overcome this problem without increasing the HRT, a nitrate shock was applied to the bioreactor by injecting the synthetic influent with a nitrate concentration of 1500 mg. L^{-1}. This shock was like a new growth in the incubation stage for the bioreactor was and applied between days 95 and 101 with a 3-hour HRT. This shock significantly increased the uptake of nutrients and the efficiency of the bioreactor, such that the effluent nitrate concentration for the 400 mg. L^{-1} influent reached 44 mg. L^{-1}, just below the standard value. Overall, the efficiency of the bioreactor was always above 50% and in a constant range of 59-68% in different HRTs for the influent with a concentration of 400 mg. L^{-1}. However, after the nitrate shock on the 104th day of the operation, a significant increase was observed in the efficiency of nitrate removal up to 87%, which can be the result of microorganism cell growth and the increased number of cells. Zhao et al. [33] also reached 90% nitrate removal efficiency in a 3-hour HRT. However, the initial concentration of nitrate and the volume of the bioreactor were much lower than in the current study.

In this work, the main concern about the effluent quality was the concentration of nitrate and nitrite ions. Therefore, these two concentrations were measured every 1 to 3 days. Fig. 9 shows the concentration profile of the input nitrate, output nitrate and output nitrite ions at different HTRs throughout the entire duration of the operation of the bioreactor. It can be seen in this figure that the amount of nitrite in the outlet was always below the standard limit (3 mg. L^{-1}), except in the growth and the nitrate shock phases. Nitrate was incompletely reduced in these phases due to the higher concentrations rather than the standard capacity of the bioreactor.
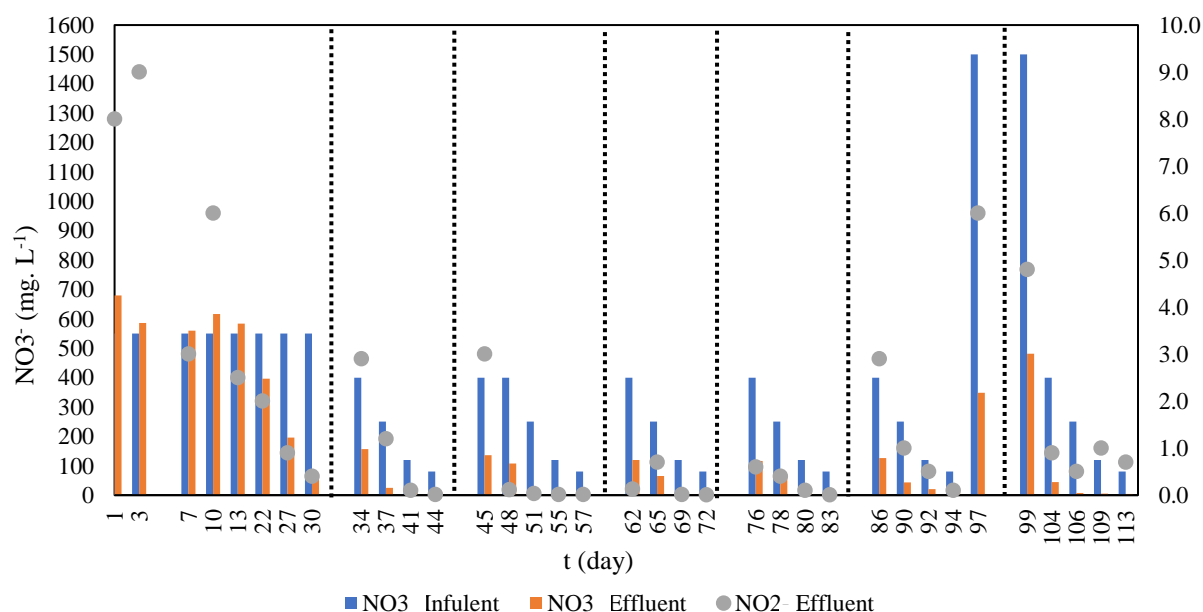
Fig. 9. Concentration of the input nitrate, output nitrate and output nitrite for different HTRs

CFD Simulations

The precision of simulation results strongly depends on the quality and size of meshes. In order to determine the proper element size, computational error of nitrate removal was calculated for each mesh size by considering the difference between experimental data and simulation results. Fig. 10 shows the error nitrate removal efficiency for different mesh sizes named by their number of elements. According to this figure, as the error does not decrease with further decreasing of the size of elements, the mesh with 155661 elements was selected for performing the simulations.
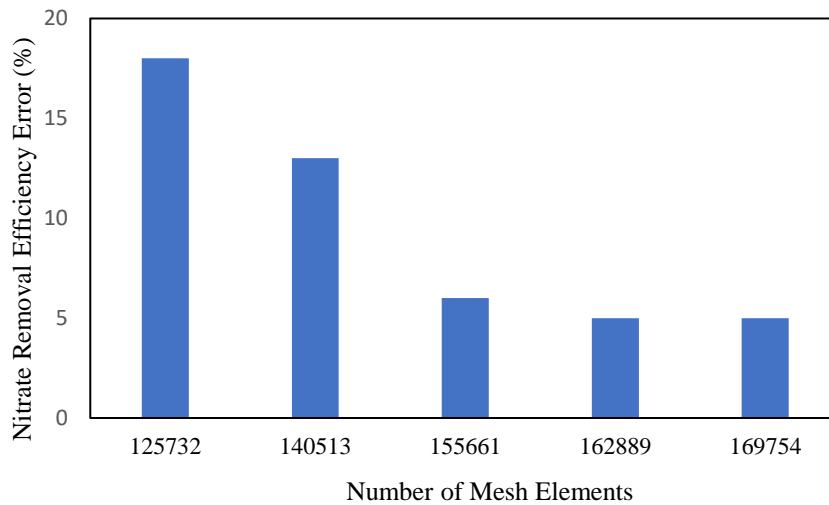
Fig. 10. Computational error based on different mesh sizes/number of elements

To ensure the reliability of CFD results, the same scenario as the experimental test was applied, with the exception that there was no need for the set-up and growth stages. An excellent agreement between the experimental data of growth rate and the prediction of Eq. (5) was observed. Maximum growth of microorganisms (μ_m) and half-velocity constant (K_s), which are shown in Table 8, were calculated through monod equation linearization [041] and applying the least-square method on nitrate concentrations at influent and effluent.

Table 8. Constants of Monod equation

μ_m (mg NO_3^- . gh^{-1})	12.7
K_s (mg NO_3^- . L^{-1})	0.47

The comparison of CFD simulation results with experiments is shown in Fig. 11. A good agreement between the experimental and simulated values can be seen in this figure and the relative error can be attributed to the environmental factors such as temperature oscillations in the experiment. Furthermore, the presence of other minerals which affect the active surface of the particles has not been taken into account in the simulations. These minerals fill the empty space of the particles and reduce the mass transfer rate for nitrate absorption.

(b) HRT= 15 Hours

■ NO3 Influent   ■ NO3 Effluent   ■ NO3 Effluent by CFD

400, 108, 106.1; 250, 16, 18.615; 120, 9, 8.9; 80, 6, 5.96

(c) HRT= 12 Hours

■ NO3 Influent   ■ NO3 Effluent   ■ NO3 Effluent by CFD

400, 157, 156.1; 250, 24, 22.622; 120, 19, 18.22; 80, 12, 10.94

(d) HRT= 10 Hours

■ NO3 Influent   ■ NO3 Effluent   ■ NO3 Effluent by CFD

400, 116, 114.27; 250, 60, 59.97; 120, 19, 20.93; 80, 2, 4.946
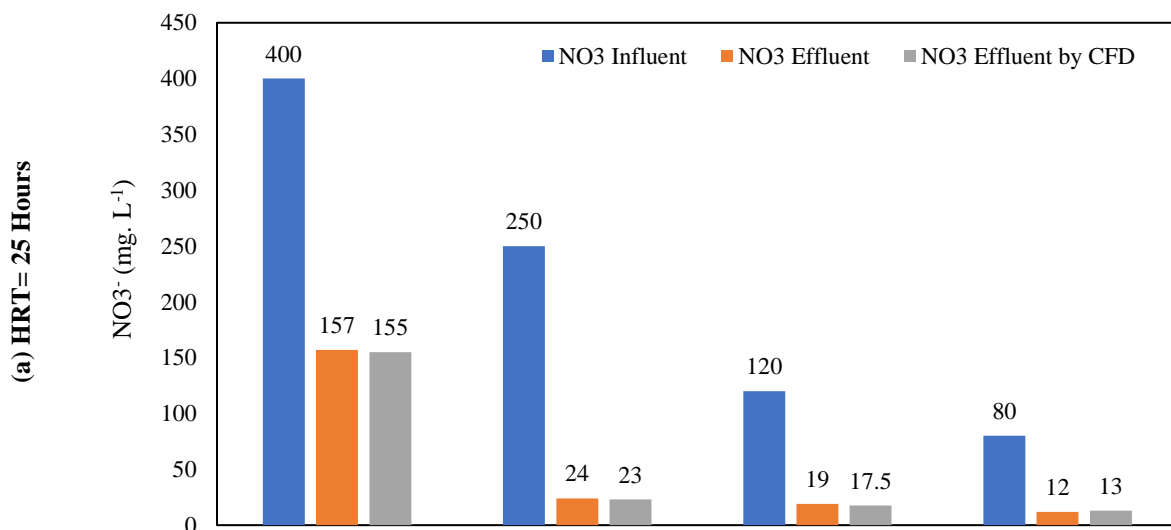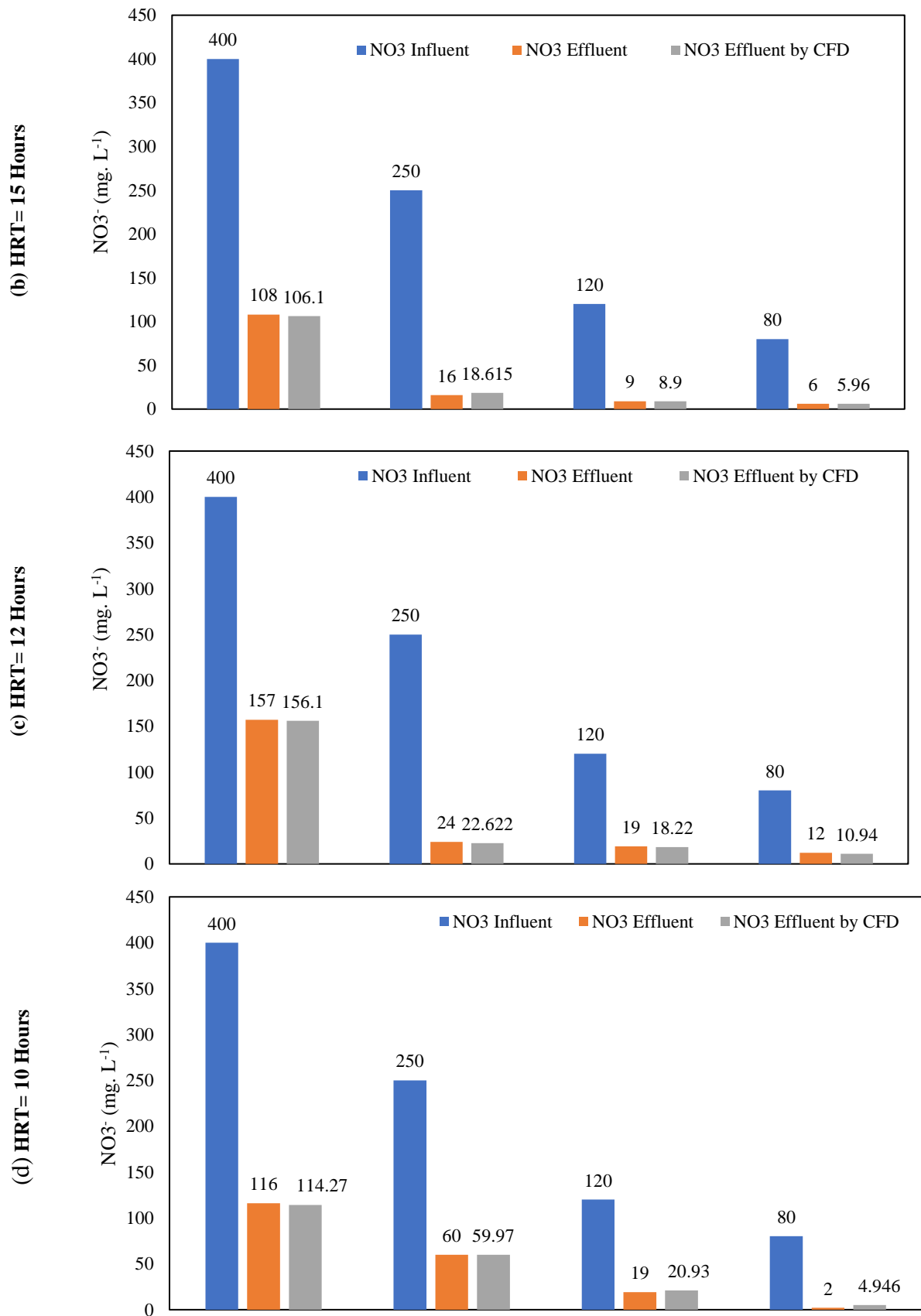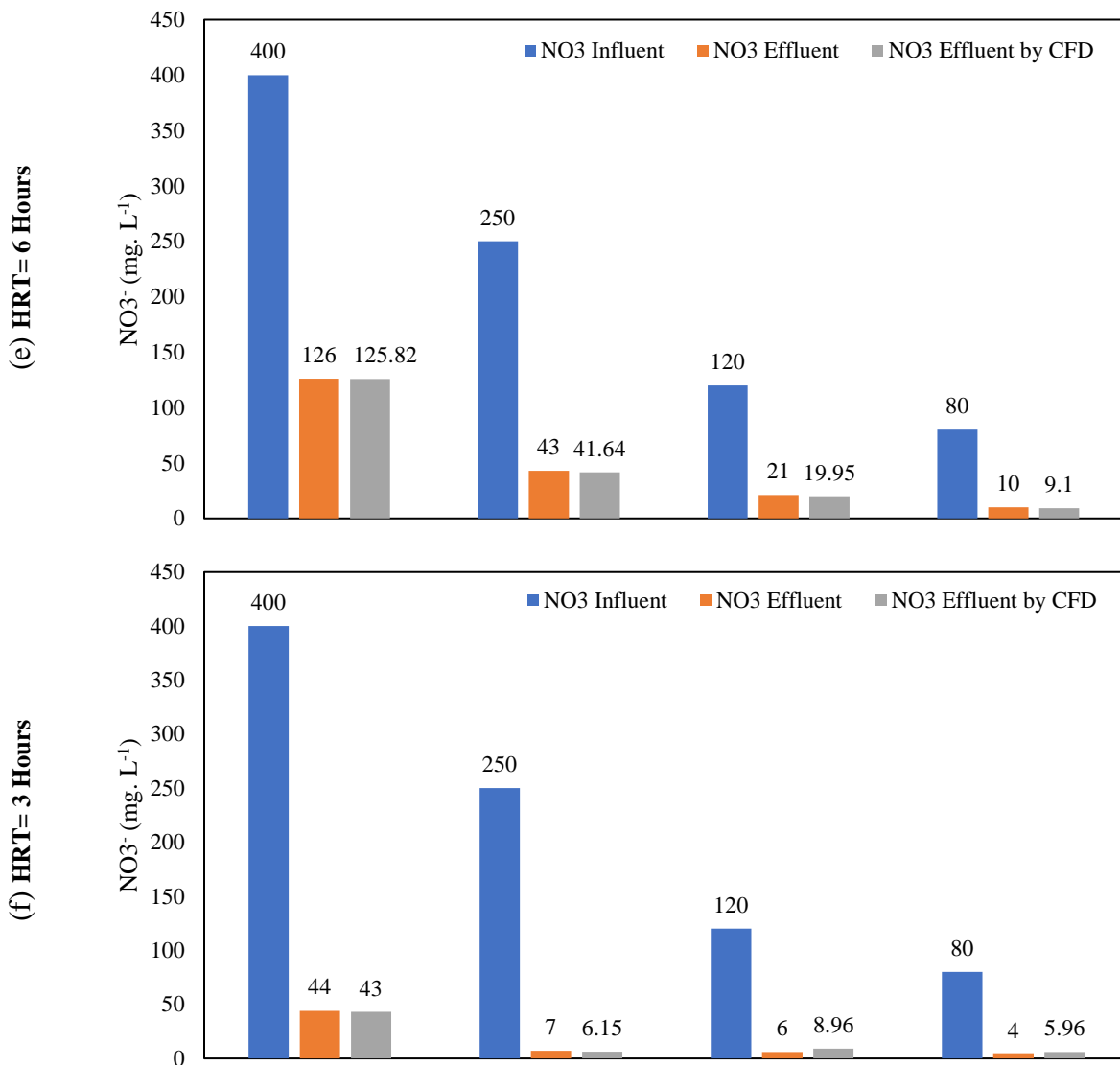
Fig. 11. Comparison of CFD simulation results with experimental measurements

Optimal Reactor Height Determination

CFD simulation was utilized for further understanding of the bioreactor performance as an alternative for the time demanding and costly experiments. Fig. 12 shows the profile of nitrate concentration along the bioreactor for various initial concentrations in the 3-hour retention time. The main purpose of this investigation is to reach the maximum nitrate removal with the minimum HRT and reactor volume. It can be seen in this figure that for the influent with 400 mg. L^{-1} nitrate concentration, the bioreactor length is optimal and the effluent concentration has reached the standard level at the end of the packed bed (90 cm). However, for the influents with 250, 120 and 80 mg. L^{-1} of nitrate concentration, the standard level could be obtained at 45, 30 and 20 cm of the reactor length.
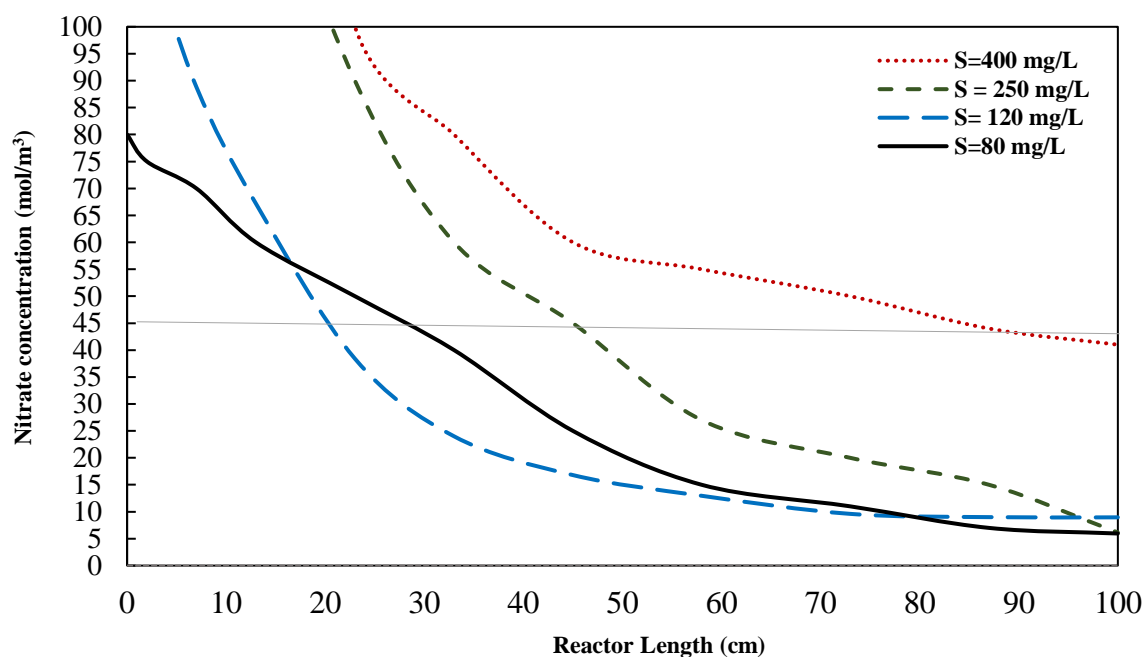
Fig. 12. Nitrate concentration along the bioreactor by simulation, HRT = 3 h

Conclusion

The effectiveness of nitrate removal was assessed in a 9.5 L packed bed column bioreactor through the evaluation of various feeding strategies and initial concentrations. The bioreactor was filled with zeolite mineral particles modified through acid washing process. Acid washing increased the pore size of zeolite particles compared to natural zeolite which facilitates the formation of microbial biofilm. Multiple hydraulic retention times were investigated to determine the efficiency of nitrate removal. The results demonstrate that the designed bioreactor is capable of achieving an 87% reduction in nitrate levels within a three-hour timeframe. This indicates that the bioreactor system can effectively remove nitrate ions from water, even when the initial nitrate content is as high as 400 mg/L, which exceeds the standard limit of 45 mg/L. The computational fluid dynamics (CFD) model yielded satisfactory results, confirming the effectiveness of the bioreactor design. It revealed that the optimal length of the bioreactor is suitable for influents containing 400 mg/L of nitrate. However, for influents with lower nitrate concentrations or when employing lower hydraulic retention times (HRTs), the bioreactor can be constructed with shorter heights. The CFD model can serve as a valuable tool for future studies, particularly in scaling up the bioreactor system.

Considering the fact that nitrate-contaminated wastewater usually contains COD, N and P simultaneously, further research is needed to investigate the performance of the presented system in this regard. Furthermore, performing microbial community analysis is highly recommended for the future works to investigate the possibility of microbial consortium instead of Thiobacillus denitrificans alone [42].

Nomenclature

Abbreviations

BSM	Basal Salt Medium
CFD	Computational Fluid Dynamics
EDX	Energy Dispersive X-ray
HRT	Hydraulic Retention Times

SEM   Scanning Electron Microscope
SW   Synthetic Water

Symbols

D_i Diffusion coefficient ($m^2 . s^{-1}$)
K   Bed permeability (s)
K_s Half-growth rate constant ($kg. m^{-3}$)
n   Normal unit vector
Q Flow rate ($m^3 . h^{-1}$)
R_i Reaction rate ($kg. m^{-3} . s^{-1}$)
r_s Concentration change ($kg/m^3 . s$)
S_i Nitrate concentration of species *i* ($kg. m^{-3}$)
S_0 Inlet nitrate concentration ($kg. m^{-3}$)
t   Time (s)
u   Velocity ($m. s^{-1}$)
u_0 Inlet velocity ($m. s^{-1}$)
V   Bed volume (m^3)

Greek letters

ε Porosity of bed
ρ Density ($kg. m^{-3}$)
μ Viscosity (Pa.s)
μ_m Specific growth rate (s^{-1})

References

[1]   Jensen VB, Darby JL, Seidel C, Gorman C. Nitrate in potable water supplies: alternative management strategies. Critical Reviews in Environmental Science and Technology. 2014;44(20):2203-86. https://doi.org/10.1080/10643389.2013.828272

[2]   Kancherla R, Kumar VR, Prabhaker Reddy G, Sridhar S. Nitrate removal studies on polyurea membrane using nanofiltration system–membrane characterization and model development. Chemical Product and Process Modeling. 2020;17(1):81-99. https://doi.org/10.1515/cppm-2020-0041

[3]   Maheswari P, Sheik AG, Tejaswini E, Ambati SR. Nested control loop configuration for a three-stage biological wastewater treatment process. Chemical Product and Process Modeling. 2020;16(2):87-100. https://doi.org/10.1515/cppm-2020-0035

[4]   Tejaswini E, Uday Bhaskar Babu G, Seshagiri Rao A. Effect of temperature on effluent quality in a biological wastewater treatment process. Chemical Product and Process Modeling. 2019;15(1):20190018. https://doi.org/10.1515/cppm-2019-0018

[5]   Rajab Beigy M, Rasekh B, Yazdian F, Aminzadeh B, Shekarriz M. High nitrate removal by starch-stabilized Fe0 nanoparticles in aqueous solution in a controlled system. Engineering in Life Sciences. 2018;18(3):187-95. https://doi.org/10.1002/elsc.201700127

[6]   Rajab Beiki M, Yazdian F, Rasekh B, Rashedi H, Darzian Rostami A. Effect of metal nanoparticles on biological denitrification process: a review. Journal of Applied Biotechnology Reports. 2016;3(1):353-8.

[7]   Rezvani F, Sarrafzadeh M-H, Ebrahimi S, Oh H-M. Nitrate removal from drinking water with a focus on biological methods: a review. Environmental Science and Pollution Research. 2019; 26:1124-41.

[8]   Sharma SK, Sobti RC. Nitrate removal from ground water: a review. E-Journal of Chemistry. 2012;9(4):1667-75. https://doi.org/10.1155/2012/154616

[9]   Ashok V, Hait S. Remediation of nitrate-contaminated water by solid-phase denitrification process—a review. Environmental Science and Pollution Research. 2015; 22:8075-93. https://doi.org/10.1007/s11356-015-4334-9

[10]   Sierra-Alvarez R, Beristain-Cardoso R, Salazar M, Gómez J, Razo-Flores E, Field JA. Chemolithotrophic denitrification with elemental sulfur for groundwater treatment. Water research. 2007;41(6):1253-62. https://doi.org/10.1016/j.watres.2006.12.039

[11]   Zhang Z, Lei Z, He X, Zhang Z, Yang Y, Sugiura N. Nitrate removal by Thiobacillus denitrificans immobilized on poly (vinyl alcohol) carriers. Journal of Hazardous Materials. 2009;163(2-3):1090-5. https://doi.org/10.1016/j.jhazmat.2008.07.062

[12]   Zhang R-C, Chen C, Xu X-J, Lee D-J, Ren N-Q. The interaction between Pseudomonas C27 and Thiobacillus denitrificans in the integrated autotrophic and heterotrophic denitrification process. Science of the Total Environment. 2022; 811:152360. https://doi.org/10.1016/j.scitotenv.2021.152360

[13]   Polizzi C, Gabriel D, Munz G. Successful sulphide-driven partial denitrification: Efficiency, stability and resilience in SRT-controlled conditions. Chemosphere. 2022; 295:133936. https://doi.org/10.1016/j.chemosphere.2022.133936

[14]   Han J, Qi X, Liang P. Improved sulfur autotrophic denitrification using supplementary bovine serum albumin. Science of The Total Environment. 2023; 859:160147. https://doi.org/10.1016/j.scitotenv.2022.160147

[15]   Koenig A, Liu L. Autotrophic denitrification of landfill leachate using elemental Sulphur. Water Science and Technology. 1996;34(5-6):469-76. https://doi.org/10.1016/0273-1223(96)00680-4

[16]   Koenig A, Liu L. Kinetic model of autotrophic denitrification in Sulphur packed-bed reactors. Water research. 2001;35(8):1969-78. https://doi.org/10.1016/S0043-1354(00)00483-8

[17]   Zhang TC, Lampe DG. Sulfur: limestone autotrophic denitrification processes for treatment of nitrate-contaminated water: batch experiments. Water Research. 1999;33(3):599-608. https://doi.org/10.1016/S0043-1354(98)00281-4

[18]   Wang H, Qu J. Combined bio electrochemical and sulfur autotrophic denitrification for drinking water treatment. Water Research. 2003;37(15):3767-75. https://doi.org/10.1016/S0043-1354(03)00249-5

[19]   Flere JM, Zhang TC. Nitrate removal with sulfur-limestone autotrophic denitrification processes. Journal of Environmental Engineering. 1999;125(8):721-9. https://doi.org/10.1061/(ASCE)0733-9372(1999)125:8(721)

[20]   Wallenstein MD, McNulty S, Fernandez IJ, Boggs J, Schlesinger WH. Nitrogen fertilization decreases forest soil fungal and bacterial biomass in three long-term experiments. Forest Ecology and Management. 2006;222(1-3):459-68. https://doi.org/10.1016/j.foreco.2005.11.002

[21]   Chen Y, Su Y, Zheng X, Chen H, Yang H. Alumina nanoparticles-induced effects on wastewater nitrogen and phosphorus removal after short-term and long-term exposure. Water research. 2012;46(14):4379-86. https://doi.org/10.1016/j.watres.2012.05.042

[22]   Kurt M, Dunn I, Bourne J. Biological denitrification of drinking water using autotrophic organisms with H2 in a fluidized-bed biofilm reactor. Biotechnology and bioengineering. 1987;29(4):493-501. https://doi.org/10.1002/bit.260290414

[23]   Montalvo S, Guerrero L, Borja R, Sánchez E, Milán Z, Cortés I, et al. Application of natural zeolites in anaerobic digestion processes: A review. Applied Clay Science. 2012; 58:125-33. https://doi.org/10.1016/j.clay.2012.01.013

[24]   Chu L, Wang J. Denitrification performance and biofilm characteristics using biodegradable polymers PCL as carriers and carbon source. Chemosphere. 2013;91(9):1310-6. https://doi.org/10.1016/j.chemosphere.2013.02.064

[25]   Yamashita T, Yamamoto-Ikemoto R, Zhu J. Sulfate-reducing bacteria in a denitrification reactor packed with wood as a carbon source. Bioresource Technology. 2011;102(3):2235-41. https://doi.org/10.1016/j.biortech.2010.10.015

[26]   Moreno-Castilla C, Bautista-Toledo I, Ferro-Garcıa M, Rivera-Utrilla J. Influence of support surface properties on activity of bacteria immobilised on activated carbons for water denitrification. Carbon. 2003;41(9):1743-9. https://doi.org/10.1016/S0008-6223(03)00123-4

[27]   Soy E, Pyeshkova V, Arkhypova V, Khadro B, Jaffrezic-Renault N, Sacco Jr A, et al. Potentialities of zeolites for immobilization of enzymes in conductometric biosensors. Сенсорна електроніка і мікросистемні технології. 2010;7(1):28-35. https://doi.org/10.18524/1815-7459.2010.1.114008

[28]   Bautista-Toledo M, Espinosa-Iglesias D, Carrasco-Marín F, Pérez-Cadenas A, Maldonado-Hódar F. Influence of the physicochemical properties of inorganic supports on the activity of immobilized bacteria for water denitrification. Journal of Environmental Management. 2015; 156:81-8. https://doi.org/10.1016/j.jenvman.2015.03.031

[29]   Philippot L. Denitrifying genes in bacterial and archaeal genomes. Biochimica et biophysica acta (BBA)-Gene structure and expression. 2002;1577(3):355-76. https://doi.org/10.1016/S0167-4781(02)00420-7

[30]   Di Capua F, Papirio S, Lens PN, Esposito G. Chemolithotrophic denitrification in biofilm reactors. Chemical Engineering Journal. 2015; 280:643-57. https://doi.org/10.1016/j.cej.2015.05.131

[31]   Abyaneh EZ, Zarghami R, Krühne U, Grundtvig IPR, Ramin P, Mostoufi N. Mixing assessment of an industrial anaerobic digestion reactor using CFD. Renewable Energy. 2022; 192:537-49. https://doi.org/10.1016/j.renene.2022.04.147

[32]   Park J-H, Shin H-S, Lee I-S, Bae J-H. Denitrification of high NO3−-N containing wastewater using elemental sulfur; nitrogen loading rate and N2O production. Environmental technology. 2002;23(1):53-65. https://doi.org/10.1080/09593332508618431

[33]   Zhao Y, Feng C, Wang Q, Yang Y, Zhang Z, Sugiura N. Nitrate removal from groundwater by cooperating heterotrophic with autotrophic denitrification in a biofilm–electrode reactor. Journal of hazardous materials. 2011;192(3):1033-9. https://doi.org/10.1016/j.jhazmat.2011.06.008

[34]   Wan D, Liu H, Qu J, Lei P, Xiao S, Hou Y. Using the combined bioelectrochemical and sulfur autotrophic denitrification system for groundwater denitrification. Bioresource technology. 2009;100(1):142-8. https://doi.org/10.1016/j.biortech.2008.05.042

[35]   Torrentó C, Cama J, Urmeneta J, Otero N, Soler A. Denitrification of groundwater with pyrite and Thiobacillus denitrificans. Chemical Geology. 2010;278(1-2):80-91. https://doi.org/10.1016/j.chemgeo.2010.09.003

[36]   Carrera J, Vicent T, Lafuente F. Influence of temperature on denitrification of an industrial high-strength nitrogen wastewater in a two-sludge system. Water Sa. 2003;29(1):11-6. https://doi.org/10.4314/wsa.v29i1.4939

[37]   Gu J-D, Qiu W, Koenig A, Fan Y. Removal of high NO3Ð concentrations in saline water through autotrophic denitrification by the bacterium Thiobacillus denitrificans strain MP. Water Science and Technology. 2004;49(5-6):105-12. https://doi.org/10.2166/wst.2004.0743

[38]   Shirazi L, Jamshidi E, Ghasemi M. The effect of Si/Al ratio of ZSM-5 zeolite on its morphology, acidity and crystal size. Crystal Research and Technology: Journal of Experimental and Industrial Crystallography. 2008;43(12):1300-6. https://doi.org/10.1002/crat.200800149

[39]   Koenig A, Liu L. Use of limestone for pH control in autotrophic denitrification: continuous flow experiments in pilot-scale packed bed reactors. Journal of Biotechnology. 2002;99(2):161-71. https://doi.org/10.1016/S0168-1656(02)00183-9

[40] Sahinkaya E, Kilic A, Duygulu B. Pilot and full-scale applications of sulfur-based autotrophic denitrification process for nitrate removal from activated sludge process effluent. Water Research. 2014; 60:210-7. https://doi.org/10.1016/j.watres.2014.04.052

[41] Kopec L, Kopec A, Drewnowski J. The application of Monod equation to denitrification kinetics description in the moving bed biofilm reactor (MBBR). International Journal of Environmental Science and Technology. 2019; 16:1479-86. https://doi.org/10.1007/s13762-018-1829-1

[42] Rezvani F, Sarrafzadeh M-H. Autotrophic granulation of hydrogen consumer denitrifiers and microalgae for nitrate removal from drinking water resources at different hydraulic retention times. Journal of Environmental Management. 2020; 268:110674. https://doi.org/10.1016/j.jenvman.2020.110674